Memorias del Congreso Nacional de Control Automático
ISSN: 2594-2492

Synchronization of Cellular Neural Networks arranged in small–world topology and signal selection for a suitable chaotic encryption

A.G. Soriano–Sánchez A.D. Cortés–Preciado
M.A. Platas–Garza A.E. Loya–Cabrera C. Elizondo–González
C. Posadas–Castillo

Universidad Autónoma de Nuevo León
Av. Pedro de Alba S/N, Cd. Universitaria, San Nicolás de los Garza,
N.L., C.P. 66455, México. (e-mail: allansori@gmail.com,
alfredo.cortespr74@gmail.com, miguel.platasg@uanl.mx,
aloya67@gmail.com, celizond@yahoo.com,
cornelio.posadascs@uanl.edu.mx).

Abstract: In this paper synchronization of a small–world network composed of Cellular Neural Networks (CNN) is addressed. Each nonlinear system used to compose the network is the standard CNN. Such model will be used as generator of chaotic behavior. The resulting small–world network will be created with Newman–Watts algorithm and synchronized by using the coupling matrix technique. On the other hand, secret communications, that includes a suitable selection of the chaotic signal as improvement of the security level, are evaluated as potential application. Criteria considering energy and frequency characteristics are used to choose the chaotic signal that best hides the message. Numerical simulations of the encryption, transmission and retrieval of a message are provided to corroborate the effectiveness of the procedure.

Keywords: Synchronization, chaotic CNN, small–world property, complex network, encryption, secret communications.

1. INTRODUCTION

In this paper, synchronization of chaos and its application are discussed. Due to the importance for engineering, in the last two decades both fields have been studied extensively.

The chaos has its beginning in the 1960's when E. Lorenz obtained the trajectories of equations describing the weather (Lorenz, 1963). As a result, many systems have been created to deepen its study. Among the chaos generators, one can find conventional chaotic oscillators (Chua et al., 1986; Lorenz, 1963), multi–scroll attractor chaotic oscillators (Yalçin, 2007), fractional–order chaotic oscillators (Petráš, 2008) and Cellular Neural Networks (Yang and Sun, 2010), for instance.

The acronym CNN for Cellular Neural Network was proposed by L.O. Chua and L. Yang in 1988 (Chua and Yang, 1998). The most remarkable characteristics of CNNs are their ability of real–time signal processing and their local interconnections (Chua and Yang, 1998; Yalçin et al., 2004).

On the other hand, chaos synchronization has its beginning in the 1990's when, L.M. Pecora and T.L. Carroll synchronized two identical chaotic oscillators with different initial conditions (Pecora and Carroll, 1990). As a result, chaotic communications have been implemented as the main application and some encryption schemes have been proposed for private communications: chaotic masking scheme (Arellano-Delgado et al., 2013), chaos shift keying scheme (Yang and Jiang, 2012) and chaotic modulation scheme (Bhat and Sudha, 2012; Wang et al., 2012), to mention a few.

Several methods have been proposed to achieve chaotic synchronization. Among the methods to achieve synchronization between coupled chaotic oscillators, one can find output synchronization (Zhang et al., 2017), the sliding modes strategy (Chen et al., 2017), synchronization through adaptive or active control (Yang et al., 2018) and Wang–Chen method (Wang and Chen, 2002b; Soriano-Sánchez et al., 2015, 2016a,b), for instance.

The last topic included in this paper is the small–world network. D.J. Watts and S.H. Strogatz suggested the first algorithm to introduce the small–world property, fulfilling two main characteristics: high clustering coefficient and short average path length (Watts and Strogatz, 1998). Some of the most recent works on this topic have shown some other important characteristics (Soriano-Sánchez and Posadas-Castillo, 2018; Bhaumik and Santra, 2017; He and Xue, 2018).

In this paper the simulation of a private communication process is performed. Firstly, some standard CNNs are arranged in small–world topology by using the Newman–Watts algorithm. The resulting complex network is synchronized through the Wang–Chen method and its dynam-

ics are considered to encrypt a message. Secondly, the resulting chaotic dynamics are evaluated to determine their energy and frequency characteristics. The chaotic signal with the best results is chosen as candidate to encrypt the message. Thirdly, the confidential message is encrypted, transmitted and retrieved to show a potential application of this topics.

The paper is organized as follows. In Section 2 the preliminaries of CNN, the model of the standard CNN, the definition of a complex networks and their synchronization are provided. Small–world networks and their main characteristics are described in Section 3. Synchronization results are provided in Section 4. Selection criteria, the encryption, transmission and retrieval of a confidential message are provided in Section 5. Some conclusions are given in Section 6

2. PRELIMINARIES

In the present section the necessary information on the standard CNN, the definition of complex network and the method to carry it to behave synchronously are provided.

2.1 The standard CNN

Among the existing definitions of CNN, authors resort to the following one, given in (Chua and Yang, 1998):

Definition 1. A Cellular Neural Network is an spatial arrangement consisting of locally–coupled cells. Each cell is a dynamical system which has an input $u(t) \in \mathbb{R}^u$, an output $y(t) \in \mathbb{R}^y$ and a state $x(t) \in \mathbb{R}^x$, evolving according to some prescribed dynamical laws.

An example of an isolated cell is given in Fig. 1.

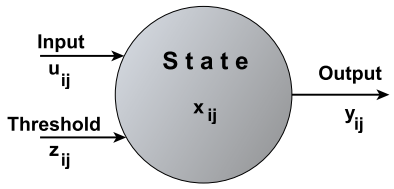

Fig. 1. A two–dimensional isolated cell: input $u_{ij}(t) \in \mathbb{R}^u$, threshold $z_{ij}(t) \in \mathbb{R}^z$, which is usually assumed to be scalar, state $x_{ij}(t) \in \mathbb{R}^x$ and output $y_{ij}(t) \in \mathbb{R}^y$.

Each cell is coupled only among the neighboring cells lying within some prescribed sphere of influence with radius r, i.e., the r–neighborhood of the cell, which is defined as follows (Chua and Yang, 1998)

$$S_r(i,j) = \{C(k,l) | \max\{|k-i|, |l-j|\} \leq r, \\ 1 \leq k \leq M, 1 \leq l \leq N\}. \quad (1)$$

Depending on the magnitude of the r–neighborhood, one can build $M \times N$ rectangular arrays of cells.

Authors will describe the standard CNN originally proposed by L.O. Chua and L. Yang in 1988 which is described as follows (Chua and Yang, 1998)

$$\dot{x}_{ij} = -x_{ij} + z_{ij} + \sum_{kl \in S_r(i,j)} a_{kl} y_{kl} \\ + \sum_{kl \in S_r(i,j)} b_{kl} v_{kl}\ , \quad i = 1, \ldots, M\ ; j = 1, \ldots, N, \quad (2)$$

and

$$y_{ij} = f(x_{ij}), \quad (3)$$

where z_{ij} is a scalar for simplicity, $S_r(i,j)$ is the sphere of influence with radius r, i.e., the r–neighborhood of the cell. $\sum_{kl \in S_r(i,j)} a_{kl} y_{kl}$ and $\sum_{kl \in S_r(i,j)} b_{kl} v_{kl}$ are the local couplings, and

$$f(x_{ij}) = \frac{1}{2}\left(|x_{ij}+1| - |x_{ij}-1|\right). \quad (4)$$

For the particular case where $M = 1$, $N = 2$, $a_{00} = 2$, $a_{0,-1} = 1.2$, $a_{01} = -1.2$, $b_{00} = 1$, $v_1(t) = 4.04sin\,(\pi t/2)$ and $v_2(t) = 0$, one obtains

$$\begin{cases} \dot{x}_1 = -x_1 + 2f(x_1) - 1.2f(x_2) + 4.04\sin\left(\frac{\pi}{2}t\right), \\ \dot{x}_2 = -x_2 + 1.2f(x_1) + 2f(x_2), \end{cases} \quad (5)$$

with the nonlinear function

$$f(x_{1,2}) = \frac{1}{2}\left(|x_{1,2}+1| - |x_{1,2}-1|\right). \quad (6)$$

It was first shown in (Zou and Nossek, 1991) that (5) – (6) exhibited chaotic behavior for the parameters given. In Fig. 2a–b the chaotic attractor and the state variables generated from (5)–(6) are shown, respectively.

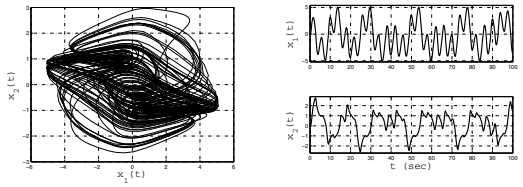

(a) (b)

Fig. 2. (**a**) View (x_1, x_2)-plane for the chaotic attractor of the standard CNN (5)–(6). (**b**) $x_1(t)$ and $x_2(t)$ state variables obtained with $\boldsymbol{x}(0) = [-0.2,\ 0.1]^T$.

2.2 Complex networks and their synchronization

Once authors have described the chaotic system to compose the network, the definition, suggested by Wang (Wang, 2002), is provided.

Definition 2. A complex network is defined as an interconnected set of oscillators (two or more), where each oscillator is a fundamental unit, with its dynamic depending on the nature of the network.

Each oscillator is defined as follows

$$\dot{\boldsymbol{x}}_i = f(\boldsymbol{x}_i) + \boldsymbol{u}_i\ , \qquad \boldsymbol{x}_i(0), \qquad i = 1,\ 2, \ldots,\ N, \quad (7)$$

where N is the size of the network, $\boldsymbol{x}_i = [x_{i1},\ x_{i2},\ \ldots,\ x_{in}] \in \mathbb{R}^{\mathrm{n}}$ represents the state variables of the oscillator i. $\boldsymbol{x}_i(0) \in \mathbb{R}^{\mathrm{n}}$ are the initial conditions for oscillator i. $\boldsymbol{u}_i \in \mathbb{R}^{\mathrm{n}}$ establishes the synchronization between two or more oscillators and is defined as follows (Wang and Chen, 2002a)

$$\boldsymbol{u}_i = c\sum_{j=1}^{N} a_{ij} \Gamma \boldsymbol{x}_j, \qquad i = 1,\ 2, \ldots,\ N. \quad (8)$$

The constant $c > 0$ represents the coupling strength. $\Gamma \in \mathbb{R}^{\mathrm{n}\times\mathrm{n}}$ is a constant matrix to determine the coupled state variable of each oscillator. Assume that following

condition for matrix $\Gamma = \text{diag}(r_1,\ r_2, \ldots,\ r_n)$ is a diagonal matrix. If two oscillators are linked through their k–th state variables, then, the diagonal element $r_k = 1$ for a particular k and $r_j = 0$ for $j \neq k$.

Synchronization is achieve through (8), where a_{ij} are the elements of $A \in \mathbb{R}^{\mathrm{N}\times\mathrm{N}}$ which is the coupling matrix. The matrix A shows the connections between oscillators; if the oscillator i–th is connected to the oscillator j–th, then $a_{ij} = 1$, otherwise $a_{ij} = 0$ for $i \neq j$. The diagonal elements of A matrix are defined as

$$a_{ii} = -\sum_{j=1, j\neq i}^{N} a_{ij} = -\sum_{j=1, j\neq i}^{N} a_{ji} \qquad i = 1, 2, ..., N. \quad (9)$$

The dynamical complex network (7)–(8) is said to achieve synchronization if

$$\boldsymbol{x}_1(t) = \boldsymbol{x}_2(t) = \ldots = \boldsymbol{x}_{\mathrm{N}}(t) \ \text{ as } \ t \to \infty. \qquad (10)$$

In this paper authors will synchronize N–coupled CNNs arranged in small–world topology.

3. NEWMAN–WATTS SMALL–WORLD ALGORITHM

In this section the small–world algorithm, used to generate the complex network, will be described. In 1999, M.E.J. Newman and D.J. Watts proposed a modified version of the original small–world model (Newman and Watts, 1999a,b).

The small–world property consists in the existence of long–range links connecting pairs of nodes distant from each other. The main features of the small–world networks are the following: on one hand *the clustering coefficient* C, which is defined as the average fraction of pairs of neighbors of a CNN that are also neighbors of each other. The clustering coefficient C_i of the CNN i is defined as the ratio between the actual number E_i of edges that exist between k_i CNNs and the total number $k_i(k_i - 1)/2$, so

$$C_i = \frac{2E_i}{k_i(k_i - 1)}. \qquad (11)$$

The clustering coefficient C of the whole network is the averaged of C_i over all i. On the other hand *the average path length* L, which is defined as the distance between two CNNs averaged over all pairs of CNNs (Wang, 2002; Barrat and Weigt, 2000)

$$L = \frac{1}{N(N-1)} \sum_{i\neq j} d_{ij}\ , \qquad 1 \leq i, j \leq N, \qquad (12)$$

where d_{ij} is the distance between CNN i and CNN j. Due to the existence of long–range links, the small–world network has high clustering coefficient $C(N, p)$ and short average path length $L(N, p)$.

When applying the Newman–Watts algorithm, authors start from the nearest neighbor topology and the small–world property is introduced by adding $N(N-(2k+1))p/2$ links to pairs of CNNs randomly chosen.

In Fig. 3 the evolution of the Newman–Watts small–world algorithm is shown. At $p = 0$ the topology remains unchanged and the network is considered regular. When $0 < p < 1$ one obtains a small–world network by adding

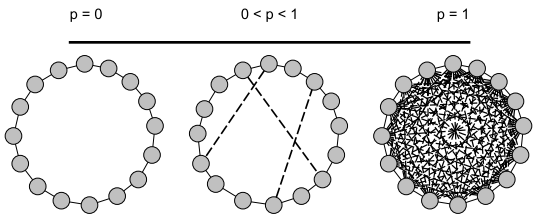

Fig. 3. Evolution of the Newman–Watts small–world algorithm. The *solid* lines are the original links. The *dash–dot* lines are the links randomly added.

links to randomly pairs of CNNs. At the point where $p = 1$ all the possible links have been added and the network has become globally coupled.

In Fig. 4 the evolution of the clustering coefficient C and the average path length L when applying the small–world algorithms is shown. When $p = 1$, Newman–Watts algorithm generates a globally coupled network whose clustering coefficient is the highest possible. i.e., every pair of CNN is connected through a link.

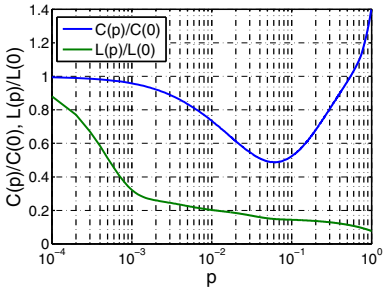

Fig. 4. Clustering coefficient C and average shortest path length L for a network generated with the Newman–Watts algorithm.

In the next section the synchronization results of the small–world network are shown.

4. SYNCHRONIZATION OF SMALL–WORLD NETWORKS

In this section authors will present the synchronization results of a small–world network. The network is composed of the standard CNN described in section 2, and it was generated by using the Newman–Watts algorithm.

4.1 Conditions for Synchronization by Using the Coupling Matrix

Suppose there are no isolated clusters in the complex network, then the coupling matrix A from section 2 is a symmetric irreducible matrix, so one eigenvalue of A is zero and all the other eigenvalues are strictly negative, this means, $\lambda_{2,\ldots,\mathrm{N}}(A) < 0$.

Theorem 1. ((Wang, 2002)). Consider the dynamical network (7). Let

$$0 = \lambda_1 > \lambda_2 \geq \lambda_3 \cdots \geq \lambda_N, \qquad (13)$$

be the eigenvalues of its coupling matrix A. Suppose that there exist an $n \times n$ diagonal matrix $H > 0$ and two constants $\bar{d} < 0$ and $\tau > 0$, such that

$$[Df(s(t)) + d\Gamma]^T H + H[Df(s(t)) + d\Gamma] \leq -\tau I_{\mathrm{n}}, \quad (14)$$

for all $d \leq \bar{d}$, where $I_{\mathrm{n}} \in \mathbb{R}^{\mathrm{n}\times\mathrm{n}}$ is an unit matrix. If moreover,

$$c\lambda_2 \leq \bar{d}, \tag{15}$$

then the synchronization state (10) is exponentially stable.

The coupling strength is computed as follows

$$c \geq \left| \frac{\bar{d}}{\lambda_2} \right|, \tag{16}$$

which will affect the stability of the synchronization state (10) through the control law (8).

4.2 Synchronization results

In the following, complex networks of identical chaotic CNNs will be synchronized. The CNNs considered is the standard CNN described by (5)–(6).

Considering a synchronization scheme of N–coupled chaotic CNN, the coupling matrix of the topology is obtained as explained in section 2. All its eigenvalues are $0 = \lambda_1 > \lambda_2 \geq \lambda_3 \ldots \geq \lambda_N$. As the small–world property is introduced, the largest nonzero eigenvalue $\lambda_2(p)$ will vary, thus, the coupling strength given by (16) becomes

$$c(p) \geq \left| \frac{\bar{d}}{\lambda_2(p)} \right|. \tag{17}$$

The coupling strength $c(p)$ is computed for each $\lambda_2(p)$, which varies depending on the small–world algorithm. The obtained ratio is the lowest boundary necessary for each type of CNN to reach synchrony and it decreases as the probability increases. Initial conditions were generated randomly for each chaotic standard CNN within the range $[-16, 10]$ without repetition. The Gamma matrix is defined such that synchronization is achieved by the first state variable, i.e., $\Gamma = \mathrm{diag}(1, 0)$. The size of the complex network is $N = 300$. The periodic boundary conditions are $k = 3$. The small–world property is introduced by Newman–Watts algorithm.

The coupling strength is computed according to (17), where $\bar{d} = -10$ and $\bar{d} = -1$ were used. According to (8), the control laws u_{i1} for $i = 1, \ldots, N$ are given by the A matrix nonzero elements for all cases. By using $\bar{d} = -10$, the chaotic state variables $x_1(t)$ and $x_2(t)$ of a single standard CNN, described by (5)–(6), are stabilized. The coupling strength c is computed from (17), thus, $c(p) \geq |-10/\lambda_2(p)|$.

The set of equations that describes the complex network is given as follows

$$\begin{cases} \dot{x}_{i1} = -x_{i1} + 2f(x_{i1}) - 1.2f(x_{i2}) \\ \qquad\quad +4.04\sin\left(\dfrac{\pi}{2}t\right) + c\displaystyle\sum_{j=1}^{N} a_{ij}x_{j1}, \\ \dot{x}_{i2} = -x_{i2} + 1.2f(x_{i1}) + 2f(x_{i2}), \end{cases} \tag{18}$$

with the nonlinear function

$$f(x_{i1,2}) = \frac{1}{2}\left(|x_{i1,2}+1| - |x_{i1,2}-1|\right), \tag{19}$$

where $1 \leq i \leq 300$. By using $p = 0.2$, the coupling strength was set in $c = 1$ and the following synchronization results were obtained. Figure 5a shows the time evolution of some chaotic state variables x_{j1} and x_{j2} for $j = 26,\ 53,\ 249,\ 130$. Figure 5b shows the phase portraits between some arbitrary chosen states and the chaotic attractor. Synchronization is confirmed by the phase portraits, therefore, condition $\boldsymbol{x}_1(t) = \boldsymbol{x}_2(t) = \ldots = \boldsymbol{x}_N(t)$ as $t \to \infty$ holds.

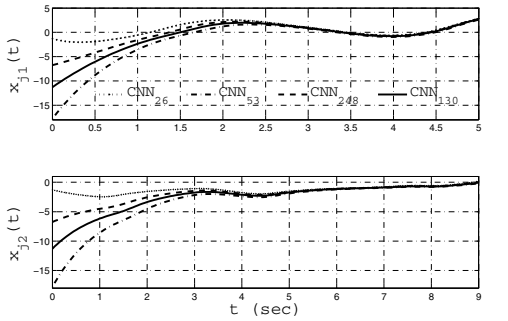

(a)

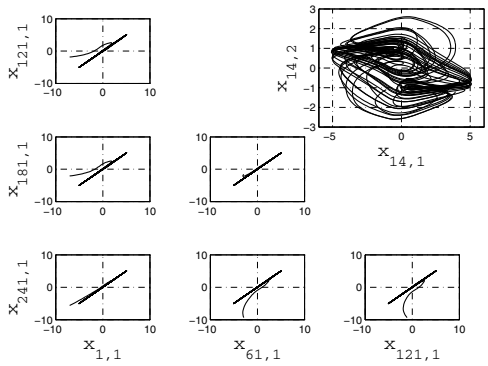

(b)

Fig. 5. (**a**) Time evolution of state variables x_{j1} and x_{j2} for $j = 26,\ 53,\ 248,\ 130$. (**b**) Phase portraits to corroborate synchronization between x_{i1} vs. x_{j1} for $i = 1,\ 61,\ 121$; $j = 121,\ 181,\ 241$ and view $(x_{14,1}, x_{14,2})$–plane of the chaotic attractor

In the next section, the simulation of a private communication system is performed. The results of the encryption, transmission and retrieval of a confidential message will be provided.

5. CHAOTIC ENCRYPTION

In this section, authors suggest criteria for assessing the energy and frequency characteristics of the chaotic signals. These data will be used to select the best chaotic signal to encrypt a confidential message.

The first criterion suggests considering the energy level of the chaotic signal. The criterion is described as follows (Soriano-Sánchez et al., 2015)

$$\sum_{n=0}^{N-1} |x_c(n)|^2 \gg \sum_{n=0}^{N-1} |x_m(n)|^2, \tag{20}$$

where $x_c(n)$ is the samples set of the chaotic signal and $x_m(n)$ is the samples set of the message (digital audio). The criterion, J_1 is defined as the ratio between the right and the left parts of (20), i.e., J_1 yields the times the chaotic signal energy exceeds the message energy, therefore, $J_1 \gg 1$ results in a good encryption.

The second criterion considers the signal energy in the frequency range where the majority of the message energy is located. This is done to ensure good encryption from the frequency domain. The criterion is described as follows (Soriano-Sánchez et al., 2015)

$$\sum_{k=0}^{N-1} \alpha(k)|X_c(k)|^2 \gg \sum_{k=0}^{N-1} \alpha(k)|X_m(k)|^2, \qquad (21)$$

where $X_c(k)$ are the chaotic signal spectrum samples, $X_m(k)$ are the message spectrum samples and $\alpha(k)$ is a frequency weighting function that selects the range where the message is located. J_2 is defined as the ratio between right and left parts of (21), which gives the relation between chaotic signal energy and message energy in a specific frequency band if $\alpha(k) = 1$ in $K \in [k_1, k_2]$. Criterion J_2 will yield how many times the weighted chaotic signal energy exceeds the weighted energy of the message, thus, $J_2 \gg 1$ results in a good encryption.

The resulting indices are given in Table 1. These data were obtained from the complex network previously synchronized. The weighting function $\alpha(k)$ has a unity gain in the message frequency range 0.01–5 kHz and null elsewhere. The total energy of the message is 3.6085×10^3.

Table 1. Indices J_1, J_2 after applying selection criteria (20) and (21) and the correlation between the message $m(t)$ and its encryption $s(t)$ in time and frequency domain $r_{m,s}$ and $R_{m,s}$ respectively. [a]Chaotic signal energy. [b] $\times 10^4$.

State	E^a	J_1	J_2	$r_{m,s}$	$R_{m,s}$
$x_{1,1}$	3.6447^b	10.1004	1.4491	0.0046	0.0118
$x_{1,2}$	0.7651^b	2.1204	2.2055	0.0067	-0.0021

5.1 Encryption results

The aim of this result is to apply the apparent randomness of chaotic systems to hide information, and use their ability to be synchronized to retrieve it. For this particular case the chaotic CNNs are arranged in small–world topology. The chaotic signal to mask the message was chosen based on its encryption capability determined by (20)–(21).

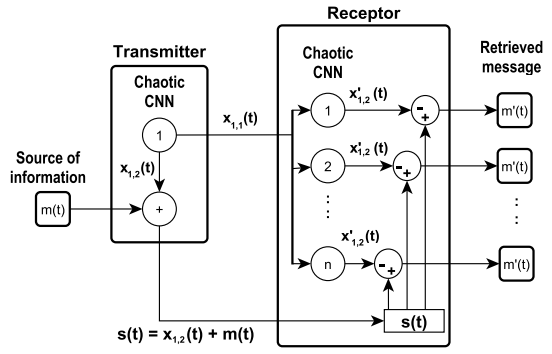

Fig. 6. Two–channel communication diagram with multi–user modality

In Fig. 6 the two–channel communication diagram with multi–user modality is shown. The additive chaotic encryption will be used to hide the confidential message. It consists on the application of autonomous chaotic oscillators whose output signal is added to the information signal. This sum is sent over a communication channel. Another chaotic signal of the encoder is also transmitted and used by the decoder to synchronize an equivalent chaotic oscillator with the encoder system. The reconstructed chaotic signal is then subtracted from the sum transmitted which finally restores the information (Dachselt and Schwarz, 2001).

Authors will consider as a confidential message a short part of the classical song *Le nozze di Figaro (The Marriage of Figaro)* by W. A. Mozart. Figure 7 shows the resulting signals of the communication process. At the top, the message to be encrypted $m(t)$; in the middle, the encrypted message $s(t) = x_{1,2}(t) + m(t)$ which is transmitted by the second channel; finally at the bottom, the retrieved message $m'(t) = s(t) - x'_{1,2}(t)$ for every user.

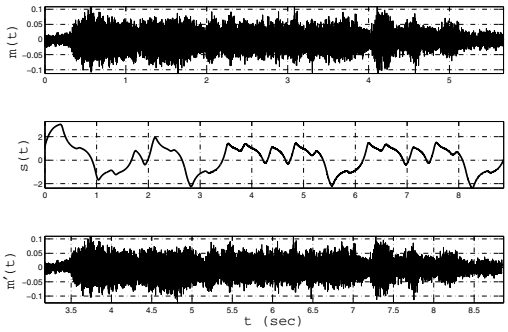

Fig. 7. Resulting signals of the communication process. At the top, the message $m(t)$ to be encrypted. In the middle the transmitted signal $s(t)$ which is the sum of the $x_{1,2}$ chaotic state and the confidential message $m(t)$. At the bottom, the retrieved message $m'(t)$

The encryption was performed by using the $x_{1,2}$ state of the standard CNN model since, as explained before, almost all its energy is located in the message frequency band. Without hesitation, selecting the chaotic signal based on its energy and bandwidth characteristics improves the security level of the encrypted message, since it is prevented from retrieval by conventional filtering techniques.

6. CONCLUSIONS

The synchronization of complex networks composed of chaotic CNN models arranged in small–world topology is highlighted. For purposes of encryption, the use of such systems allows us to generate a wide variety of chaotic signals, which makes the selection process more effective, since the greater the number of signals evaluated, more extensive is the field of requirements that can be met.

The use of criteria to select the chaotic signal to hide the message, which consider energy and frequency characteristics, is without hesitation the most remarkable contribution of the paper, due to it brings an improvement in the security level of the encrypted message. Authors have shown the importance of knowing the message bandwidth to choose a suitable chaotic signal. The encrypted mes-

sage is prevented from being retrieved by using filtering techniques.

ACKNOWLEDGEMENTS

This work was supported by CONACYT México under research Grant No. 166654, PAICyT under research grant IT640-18 and Facultad de Ingeniería Mecánica y Eléctrica (FIME–UANL).

REFERENCES

Arellano-Delgado, A., López-Gutiérrez, R., Cruz-Hernández, C., Posadas-Castillo, C., Cardoza-Avendano, L., and Serrano-Guerrero, H. (2013). Experimental network synchronization via plastic optical fiber. *Opt. Fiber Technol.*, 19(2), 93–108.

Barrat, A. and Weigt, M. (2000). On the properties of small–world network models. *Eur. Phys. J. B*, 13, 547–560.

Bhat, L. and Sudha, K.L. (2012). Performance analysis of chaotic DS–CDMA with CSK modulation. *Int. J. Adv. Eng. Res. Stud.*, 1(3), 133–136.

Bhaumik, H. and Santra, S. (2017). Stochastic sandpile model on small-world networks: scaling and crossover. *arXiv preprint arXiv:1710.08741*.

Chen, X., Park, J.H., Cao, J., and Qiu, J. (2017). Sliding mode synchronization of multiple chaotic systems with uncertainties and disturbances. *Appl. Math. Comput.*, 308, 161–173.

Chua, L.O., Komuro, M., and Matsumoto, T. (1986). The Double Scroll Family. *IEEE Trans. Circuits Syst.*, 11, 1072–1118.

Chua, L.O. and Yang, L. (1998). Cellular Neural Networks: Theory and applications. *IEEE Trans. Circuits Syst.*, 35, 1257–1290.

Dachselt, F. and Schwarz, W. (2001). Chaos and cryptography. *IEEE Trans. Circuits Syst.-I: Fundam. Theory Appl.*, 48, 1498–1509.

He, J. and Xue, Y. (2018). Scale-free and small-world properties of hollow cube networks. *Chaos, Solitons Fract.*, 113, 11–15.

Lorenz, E.N. (1963). Deterministic Nonperiodic Flow. *J. Atmos. Sci.*, 20, 130–141.

Newman, M.E.J. and Watts, D.J. (1999a). Renormalization group analysis of the small–world network model. *Phys. Lett. A*, 263, 341–346.

Newman, M.E.J. and Watts, D.J. (1999b). Scaling and percolation in the small–world network model. *Phys. Rev. E*, 60, 7332–7342.

Pecora, L.M. and Carroll, T.L. (1990). Synchronization in chaotic systems. *Phys. Rev. Lett.*, 64, 821–824.

Petráš, I. (2008). A note on the fractional–order Chua's system. *Chaos, Soliton Fract.*, 38, 140–147.

Soriano-Sánchez, A.G., Posadas-Castillo, C., Platas-Garza, M.A., Cruz-Hernández, C., and López-Gutiérrez, R.M. (2016a). Coupling strength computation for chaotic synchronization of complex networks with multi–scroll attractors. *Appl. Math. Comput.*, 275, 305–316.

Soriano-Sánchez, A.G., Posadas-Castillo, C., Platas-Garza, M.A., and Diaz-Romero, D.A. (2015). Performance improvement of chaotic encryption via energy and frequency location criteria. *Math. Comput. Simul.*, 112, 14–27.

Soriano-Sánchez, A.G., Posadas-Castillo, C., Platas-Garza, M.A., and Diaz-Romero, D.A. (2015). Performance improvement of chaotic encryption via energy and frequency location criteria. *Math. Comput. Simul.*, 112, 14–27.

Soriano-Sánchez, A.G., Posadas-Castillo, C., Platas-Garza, M.A., and Elizondo-González, C. (2016b). Chaotic synchronization of cnns in small–world topology applied to data encryption. In *Advances and Applications in Chaotic Systems*, 337–362. Springer.

Soriano-Sánchez, A. and Posadas-Castillo, C. (2018). Smart pattern to generate small–world networks. *Chaos, Solitons Fract.*, 114, 415–422.

Wang, M.J., Wang, X.Y., and Pei, B.N. (2012). A new digital communication scheme based on chaotic modulation. *Nonlinear Dyn.*, 67(2), 1097–1104.

Wang, X.F. (2002). Complex Networks: Topology, Dynamics and Synchronization. *Int. J. Bifurc. Chaos*, 12(5), 885–916.

Wang, X.F. and Chen, G. (2002a). Synchronization in small–world dynamical networks. *Int. J. Bifurc. Chaos*, 12(1), 187–192.

Wang, X.F. and Chen, G. (2002b). Synchronization in small–world dynamical networks. *Int. J. Bifurc. Chaos*, 12(1), 187–192.

Watts, D.J. and Strogatz, S.H. (1998). Collective dynamics of small–world networks. *Nature*, 393, 440–442.

Yalçin, M.E. (2007). Multi–scroll and hypercube attractors from a general jerk circuit using Josephson junctions. *Chaos, Soliton Fract.*, 34, 1659–1666.

Yalçin, M.E., Suykens, J.A.K., and Vandewalle, J.P.L. (eds.) (2004). *Cellular Neural Networks, Multi–Scroll Chaos and Synchronization*, volume 50 of *Serie A*. World Scientific, Singapore.

Yang, H. and Jiang, G.P. (2012). High–Efficiency Differential–Chaos–Shift–Keying Scheme for Chaos–Based Noncoherent Communication. *IEEE Trans. Circuits Syst.–II: Express Briefs*, 59(5), 312–316.

Yang, H., Wang, X., Zhong, S., and Shu, L. (2018). Synchronization of nonlinear complex dynamical systems via delayed impulsive distributed control. *Appl. Math. Comput.*, 320, 75–85.

Yang, W. and Sun, J. (2010). Function projective synchronization of two-cell quantum-CNN chaotic oscillators by nonlinear adaptive controller. *Phys. Lett. A*, 374(4), 557–561.

Zhang, Z.M., He, Y., Wu, M., and Wang, Q.G. (2017). Exponential synchronization of chaotic neural networks with time-varying delay via intermittent output feedback approach. *Appl. Math. Comput.*, 314, 121–132.

Zou, F. and Nossek, J.A. (1991). A Chaotic Attractor with Cellular Neural Networks. *IEEE Trans. Circuits Syst.*, 38(7), 811–812.

